[w, δ(CH)], 1349 [vw, ν(CN)], 1322 [vw, δ(CH)], 1298 [vw, δ(C–O–CH$_2$) [b]], 1196 [w, δ(CO)], 1119 [m, ν(C–C=O) [b]], 1053 [w, ν(SiO)], 962 [w, ν(WO)], 926 [w, ν(WO)], 902 [w, ν(WO)], 866 [w, ν(WO)], 820 [w, ν(WO)], 749 [w, ν(WO)], 627 [vs, ν(FeO)], 561 [vs, ν(FeO)].

The BA ferrogels were prepared under the same conditions as the POM ferrogels but replacing POM by *N,N′*-methylenebis(acrylamide) (BA) (0.017, 0.042, and 0.084 mol/L). The infrared data of a BA ferrogel with 0.017 M of BA and 5.5 % (volume fraction) of maghemite γ-Fe$_2$O$_3$: IR (KBr): ν = 1665 [s, ν(CO) [a]], 1615 [s, δ(NH)], 1448 [m, δ(CH$_2$)], 1414 [m, δ(CH)], 1349 [m, ν(CN)], 1322 [w, δ(CH)], 1119 [vw, ν(C–C=O) [b]], 627 [vs, ν(FeO)], 561 [vs, ν(FeO)].

Physical Measurements: The compound γ-K$_8$[SiW$_{10}$O$_{36}$]·12H$_2$O was prepared according to the literature [16]. Other reagents, [RSi(OMe)$_3$], and solvents were purchased from Aldrich and used as received. Elemental analyses were performed by the "Service central de microanalyses du CNRS", Vernaison, France. The IR spectra (4000–250 cm^{-1}) were recorded on a Bio-Rad FTS 165 FTIR spectrometer with compounds and dried hydroferrogels sampled in KBr pellets. The volume fraction of magnetic particles in the different hydroferrogels and the particle sizes are deduced from magnetic measurements using a classical Foner device [17]. The rotational diffusion coefficient of particles is determined by the relaxation of birefringence. This method has already been described in the literature [15]. Transmission electron microscopy (TEM) (microscope JEOL 100 CX2) was performed on a microcoat of hydroferrogel deposited on a grid after microtomy. The gels are filmed with a charge coupled device (CCD) color camera (Vista, VPC 4130, UK). The degree of swelling of the hydroferrogel samples was characterized by the ratio m/m_0, where m is the mass of the hydroferrogel sample swollen in aqueous solution and m_0 is the mass of the dry hydroferrogel.

Received: October 13, 1999

[1] W. S. Stoy, F. J. Washabaugh, in *Encyclopedia of Polymer Science and Engineering,* 2nd ed. (Eds: H. F. Mark, N. M. Bikales, C. G. Overberger, G. Mendes), Wiley , New York **1987**, Vol. 7, p. 53.
[2] M. Sadakane, E. Steckhang, *Chem. Rev.* **1998**, *98*, 219.
[3] G. Bidan, O. Jarjayes, J. M. Fruchart, E. Hannecart, *Adv. Mater.* **1994**, *6*, 152.
[4] M. Zrinyi, L. Barsi, D. Szabo, *J. Chem. Phys.* **1997**, *106*, 5685.
[5] M. Zrinyi, L. Barsi, A. Büki, *J. Chem. Phys.* **1996**, *104*, 8750.
[6] R. Massart, *IEEE Trans Magn. Mater.* **1981**, *17*, 131.
[7] V. Cabuil, R. Massart, *J. Chem. Phys.* **1987**, *84*, 967.
[8] R. Massart, E. Dubois, V. Cabuil, E. Hasmonay, *J. Magn. Magn. Mat.* **1995**, *149*, 1.
[9] J. C. Bacri, R. Perzynski, D. Salin, *J. Magn. Magn. Mat.* **1988**, *71*, 246.
[10] J. C. Bacri, R. Perzynski, D. Salin, V. Cabuil, R. Massart, *J. Magn. Mater.* **1990**, *85*, 27.
[11] C. R. Mayer, I. Fournier, R. Thouvenot, *Chem. Eur. J.* **2000**, *6*, 105.
[12] M. Mandel, "Polyelectrolytes", in *Encyclopedia of Polymer Science and Engineering*, 2nd ed. (Eds: H. F. Mark, N. M. Bikales, C. G. Overberger, G. Mendes), Wiley, New York **1988**, Vol. 11, p. 739.
[13] E. Philippova, O. E. Philippova, R. Rulkens, B. I. Kovtunenko, S. S. Abramchuk, A. R. Khokhlov, G. Wegner, *Macromolecules* **1998**, *31*, 1168.
[14] S. L. Shenoy, *J. Polym. Sci., Part B: Polym. Phys.* **1998**, *36*, 2525.
[15] J. C. Bacri, V. Cabuil, R. Massart, R. Perzynski, D. Salin, *J. Magn. Magn. Mater.* **1987**, *65*, 285.
[16] J. Canny, A. Tézé, R. Thouvenot, G. Hervé, *Inorg. Chem.* **1986**, *25*, 2114.
[17] S. Foner, E. J. Macniff Jr., *Rev. Sci. Instrum.* **1968**, *39*, 171. J. C. Bacri, R. Perzynski, D. Salin, V. Cabuil, R. Massart, *J. Magn. Magn. Mater.* **1986**, *62*, 36.

Electrical Transport Through Individual Vanadium Pentoxide Nanowires**

By *Jörg Muster,* Gyu Tae Kim, Vojislav Krstić, Jin Gyu Park, Yung Woo Park, Siegmar Roth,* and *Marko Burghard*

One-dimensional nanostructures, such as chemically synthesized nanowires or nanotubes, are of considerable interest as functional units mediating the transport of electrons or optical excitations. Probing their intrinsic properties is critical to assess their possible role in new types of nanoscale devices. In this context, carbon nanotubes (CNTs) are currently being investigated in great detail. These remarkable molecular objects were shown to behave as ballistic nanowires able to sustain very high current densities.[1] In addition, model nanodevices such as field-effect transistors have been fabricated from individual single-wall nanotubes.[2,3] However, CNTs exist in different chiralities and diameters, corresponding to metallic or semiconducting tubes with band gaps of up to ~0.8 eV.[4] Although some control over the tube diameter has been achieved during synthesis on patterned substrates,[5] no procedure is available to obtain pure tubes of one specific type. Therefore nanowires that are more homogeneous in structure are of importance. Possible alternatives include nanotubes of WS_2,[6,7] silicon nanowires,[8] nucleic acid strands,[9] or scroll-like vanadium pentoxide nanotubes.[10] Here we present the controlled deposition and electrical properties of individual vanadium pentoxide (V_2O_5) nanowires, which possess a ribbon-like structure and are 1.5 nm in height, 10 nm in width, and up to a few micrometers long. It is well known that V_2O_5 fibers are obtained by polycondensation of vanadic acid in water.[11] Due to the strongly anisotropic structure of the fibers, sols prepared in this manner exhibit a number of remarkable properties, including liquid-crystalline behavior.[12] Vanadium pentoxide sols/gels have nowadays found application in the photographic industry as antistatic coatings.[13] The internal structure of the V_2O_5 fibers was resolved only a few years ago by X-ray diffraction[14] and cryo-transmission electron microscopy (cryo-TEM).[15] These studies revealed a double layer structure of the fibers, with each layer consisting of two V_2O_5 sheets,

[*] J. Muster, V. Krstić, Dr. S. Roth, Dr. M. Burghard
Max-Planck-Institut für Festkörperforschung
Heisenbergstrasse 1, D-70569 Stuttgart (Germany)
G. T. Kim, J. G. Park, Prof. Y. W. Park
Department of Physics and Condensed Matter Research Institute
Seoul National University, Seoul 151-742 (Korea)

[**] The authors are grateful to F. Schartner, U. Waizmann, and M. Riek for technical support. This work was supported by the KISTEP program of the Ministry of Science and Technology in Korea (contract No. 98-I-01-04-A-026). Partial support for G. T. K. was received from the KOSEF research training fellowship program in Germany. M. B. thanks the Deutsche Forschungsgemeinschaft (DFG) for financial support.

  0935-9648/00/0603-0420 $ 17.50+.50/0

ADVANCED MATERIALS

as depicted in Scheme 1. It is noteworthy that a V_2O_5 fiber is composed of only four atomic layers of vanadium, which therefore represents a wire with a thickness of molecular dimension. Several studies of the electrical transport in bulk V_2O_5, such as amorphous[16] and crystalline material[17] as well as V_2O_5 xerogels,[18] have been published. However, to our knowledge, no electrical transport data on individual V_2O_5 fibers have been reported up to now.

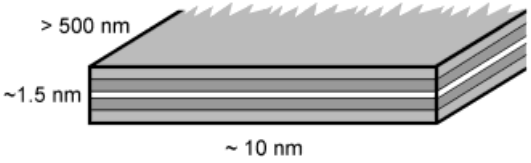

Scheme 1. Schematic representation of an individual V_2O_5 fiber consisting of 4 sheets of V_2O_5 arranged in a double layer structure.

The V_2O_5 sols used in the present study were prepared from ammonium (meta)vanadate in the presence of an acidic ion exchanger, adopting a procedure reported by Gharbi and coworkers.[19] The surface of the V_2O_5 fibers is covered by hydroxyl groups, which dissociate in aqueous media. As a result, at pH 2 on average a partial charge of about –0.3 is carried by each V_2O_5 unit.[11] Taking advantage of this negative surface charge, individual V_2O_5 fibers can be deposited onto appropriately modified Si/SiO_2 surfaces. For that purpose, the SiO_2 surface is first treated with 3-aminopropyltriethoxysilane (3-APS) to create positively charged ammonium groups on the surface. The ionic interaction between the negatively charged V_2O_5 fibers and the positively charged SiO_2 surface then allows a controlled adsorption process. Deposition of only a few single V_2O_5 fibers was achieved by optimization of the sol concentration (2 mM) and adsorption time (2–3 s).

Detailed structural investigations of the V_2O_5 fibers were performed by scanning force microscopy (SFM). A representative SFM image of a substrate covered with individual fibers is shown in Figure 1a, and a more detailed image of two fibers on a substrate with a lower density of fibers is shown in Figure 1b. Figure 1c shows the cross-sectional analysis along the line in Figure 1b, from which the height of the fibers is found to be 1.5 nm. This value is in excellent agreement with the data obtained from cryo-TEM investigations.[15] Heights of twice or three times 1.5 nm, which indicate the presence of condensed V_2O_5 fibers, were observed only for small fractions of the fibers. On the other hand, the measured width of ~20–40 nm is considerably larger than the value of 10 nm obtained by TEM investigations. This difference is attributed to the tip-convolution characteristic of the SFM technique.[20]

Samples for electrical transport measurements were prepared by a procedure similar to that employed for the deposition of V_2O_5 fibers onto bare SiO_2 surfaces. In order to get an initial impression of the conductivity of adsorbed fibers, we performed electrical measurements on thin (~10 nm average thickness) networks of V_2O_5 fibers on electrode arrays with electrodes separated by about 3 µm.

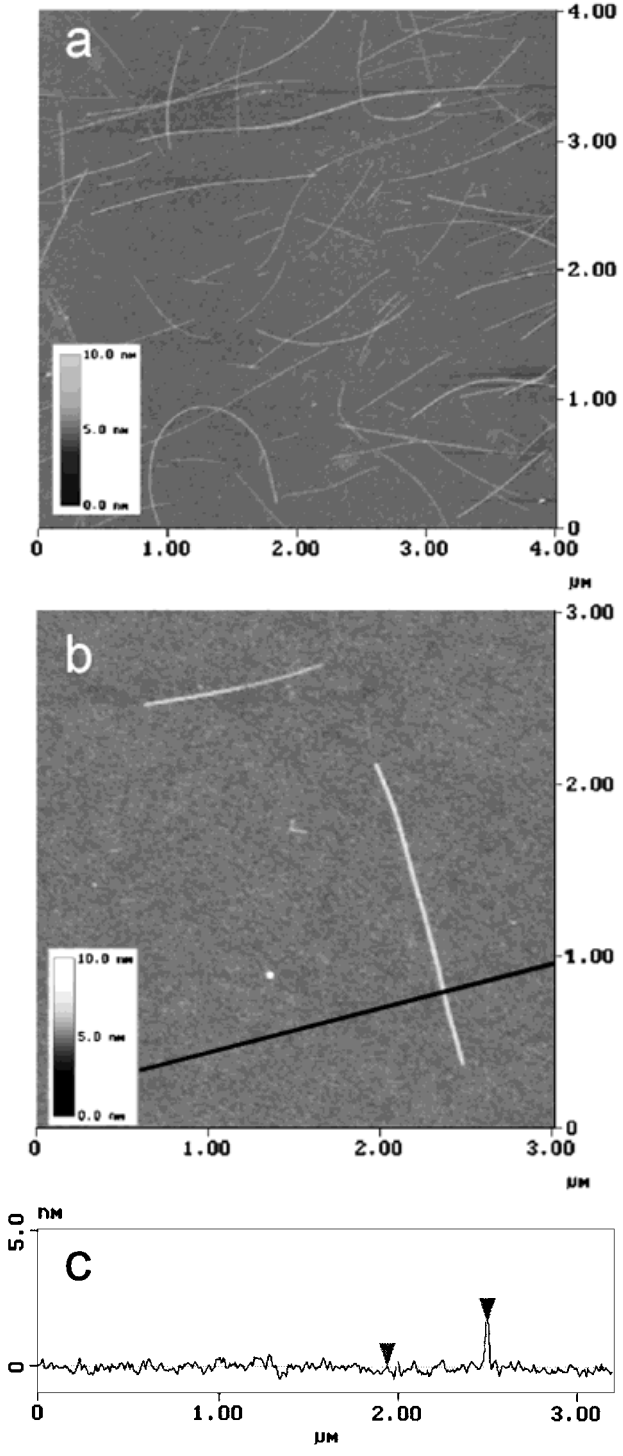

Fig. 1. a) Representative SFM image of individual V_2O_5 fibers adsorbed on an aminosilanized SiO_2 surface. b) SFM image of two well-separated V_2O_5 fibers. c) Cross-sectional analysis along the line in (b), revealing a fiber height of 1.5 nm.

Such networks were deposited on aminosilanized substrates using adsorption times of several minutes and a V_2O_5 sol concentration of ~20 mM. At room temperature, the samples exhibited slightly nonlinear, symmetric current/voltage (I/V) characteristics, as exemplified in Figure 2b for the specific network shown in Figure 2a. From

  0935-9648/00/0603-0421 $ 17.50+.50/0

various samples, a contact resistance of 0.5–1.0 kΩ was derived by comparison between 2- and 4-probe measurements. Because the effective cross-section of the sample is not exactly known, the conductivity of the network (Fig. 2a) can only be estimated to fall in the range ~ 0.1–1 S/cm at room temperature. Such a high conductivity, as compared to vapor deposited V_2O_5 ($\sigma \sim 10^{-6}$ S/cm[21]) or rf-sputtered V_2O_5 ($\sigma \sim 10^{-4}$–10^{-3} S/cm[22]), has also been reported for much thicker films of gel-derived V_2O_5.[23,24] It is generally accepted that electrical conduction in V_2O_5 xerogels proceeds via hopping between V^{5+} and V^{4+} impurity centers. Depending on the preparation method, the amount of V^{4+} can reach up to 10 % of the total amount of vanadium atoms in the sample.[25] Temperature dependent measurements revealed a decline in conductivity with decreasing temperature, consistent with thermally activated hopping transport. The resistance R of the thin network is plotted in Figure 2c as $\ln(T/R)$ versus reciprocal temperature in the range of 80–300 K. This plot is performed to analyze the data in the frame of the general formula proposed by Mott[26] for small polaron hopping in transition metal oxides:

$$\sigma = (v_0 e^2 C(1-C) / kTr) \exp(-2\alpha r) \exp(-W / kT) \quad (1)$$

where v_0 is a phonon frequency, C the concentration ratio $V^{4+}/(V^{4+} + V^{5+})$, r the average hopping distance, W the activation energy, and α the rate of wave function decay. The pronounced departure from linearity of the $\ln(T/R)$ versus $1/T$ plot in Figure 2c is in accordance with the observation of Bullot and coworkers, who investigated thick amorphous V_2O_5 layers deposited from gels.[24] This behavior has been explained by the temperature dependence of the hopping activation energy W, which includes a disorder energy W_d attributed to the random structure of the material. Approximating the plot (Fig. 2c) by a straight line in the high temperature range ($T > 222$ K) leads to an activation energy of 0.21 eV, which falls in the range of 0.2–0.4 eV reported by other groups.[25]

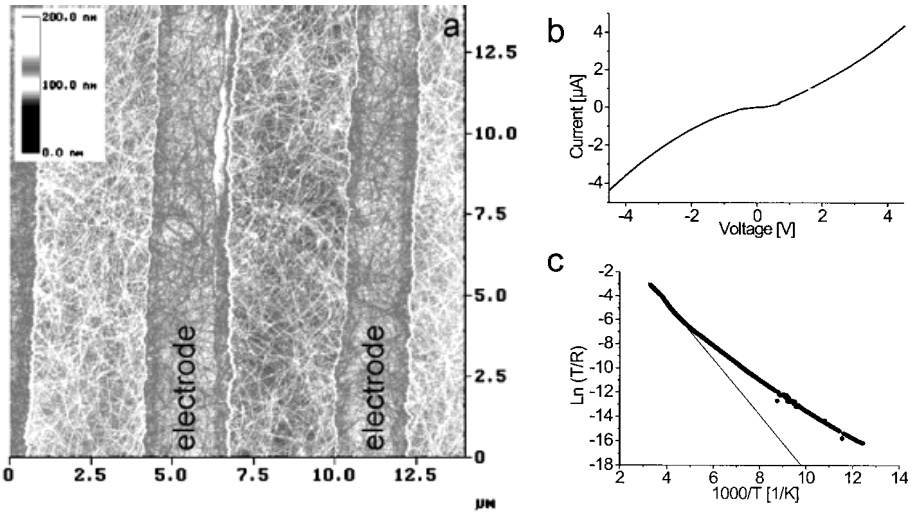

Fig. 2. a) SFM image of a thin V_2O_5 network deposited on an electrode array with 3 µm electrode separation. b) I/V characteristic of the sample at room temperature. c) Temperature dependence of network resistance.

Following the electrical characterization of thin network samples, individual V_2O_5 fibers were deposited on prefabricated electrode arrays with electrode separation of ca. 100 nm. The SFM image of a typical sample is presented in Figure 3a. In this specific case, two V_2O_5 fibers are in contact with the left-hand electrode pair, which shows a nonlinear, symmetric I/V characteristic at room temperature (Fig. 3b). Application of 0.5 V bias resulted in a current in the range of 2 pA, whereas at liquid helium temperature a measurable current (exceeding ~ 0.5 pA) required a bias >3.5 V (Fig. 3c). The increased resistance at low temperatures can be explained by an increased resistivity of the fibers (thermally activated hopping) and/or an increased contact resistance. Due to this high total resistance reliable 4-probe conductivity measurements, which would allow separation of the intrinsic fiber resistance from the contact resistance, could not be performed. However, in view of

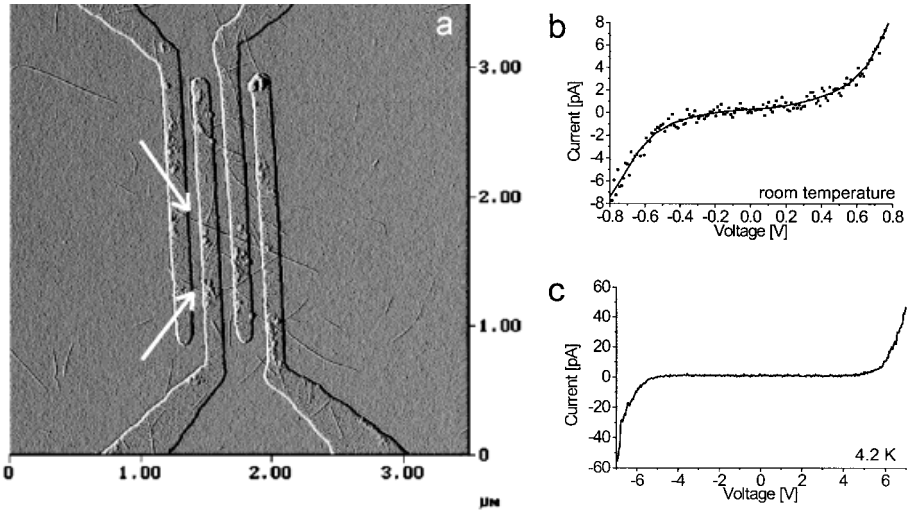

Fig. 3. a) SFM amplitude image showing two individual V_2O_5 fibers (marked by arrows) on top of the left electrode pair. b) I/V characteristic of the two fibers at room temperature; experimental data (dotted line), fit (solid line). c) I/V characteristic at 4.2 K.

0935-9648/00/0603-0422 $ 17.50+.50/0

ADVANCED MATERIALS

the high contact resistance reported for, e.g., carbon nanotubes deposited on electrodes,[27] we note that an adsorbate layer on the AuPd surface could significantly contribute to the observed high resistance. In order to avoid these problems in subsequent experiments, AuPd electrodes were lithographically deposited over V_2O_5 fibers adsorbed on an aminosilanized Si/SiO_2 wafer. After electrode deposition, no change in the structure of the fibers was apparent from SFM investigations. A sample prepared in this way is shown in the SFM image of Figure 4a. The 2- and 4-probe *I*/*V* characteristic of the five fibers in contact with the middle electrode pair is displayed in Figure 4b as dotted and solid line, corresponding to a resistance of 48.2 MΩ and 27.8 MΩ, respectively. Obviously, a much lower, ohmic resistance is achieved through this contact configuration. Assuming that the four electrodes make identical electrical contacts to the fibers, and taking a total cross-section of 75 nm^2 (5 × 1.5 nm × 10 nm), the conductivity of one single fiber reaches ~ 0.5 S/cm at room temperature. This value is in the range estimated above for the fiber network. The fact that the conductivity of the individual fibers is not larger than the network conductivity could be due to a reduced carrier concentration in the fibers. One possible origin for carrier depletion is electron transfer from the V_2O_5 fibers to the AuPd electrodes (possessing a relatively high work function), which should be larger in case of the intimate contact between the metal and individual fibers. The temperature dependence of 4-probe resistance is displayed in Figure 4c, with the inset showing the plot according to the small polaron hopping model described above. In contrast to the network sample (see Fig. 2c), the plot is linear over the full temperature range of 110–300 K. From the slope of the line, an activation energy of 0.11 eV is calculated, which is significantly smaller than the value of 0.21 eV obtained for the network sample. We attribute both the small value of the activation energy and the linearity of the ln(*T*/*R*) versus 1/*T* plot to the fact that the transport through the individual fibers is not influenced by inter-fiber contacts, as predicted by Bullot and coworkers.[24]

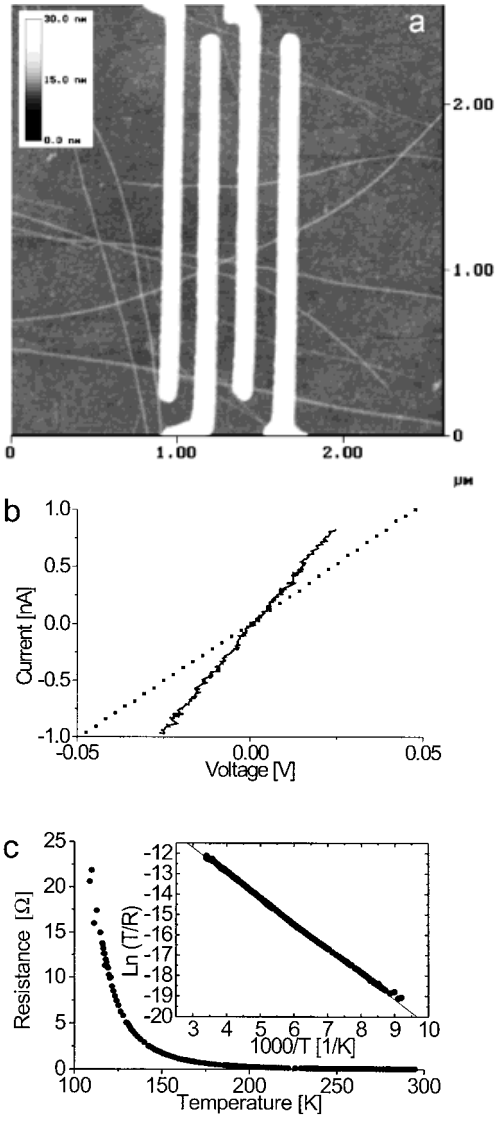

Fig. 4. a) SFM image of AuPd electrodes patterned on vanadium pentoxide fibers. The electrodes are separated by about 150 nm. b) 2-probe (dotted line) and 4-probe (solid line) *I*/*V* characteristic at room temperature. The 2-probe measurement was performed with the middle electrode pair. c) Temperature dependence of 4-probe resistance *R*. The inset shows a plot of ln(*T*/*R*) versus 1000/*T*.

In conclusion, individual V_2O_5 fibers were successfully deposited on chemically modified SiO_2 substrates allowing detailed SFM studies to be carried out. The obtained fiber dimensions are in good agreement with the TEM results reported by Bailey and coworkers.[15] Electrical conduction through thin (~10 nm) V_2O_5 networks was found to behave similarly to thicker (0.1–1 μm) V_2O_5 xerogels. Individual V_2O_5 fibers deposited on prefabricated electrodes revealed nonlinear *I*/*V* characteristics with high resistance. Increased conductivity was achieved by deposition of AuPd electrodes on top of the fibers. The conductivity of one individual V_2O_5 fiber was estimated to be ~0.5 S/cm at room temperature. Compared to the fiber networks, the individual fibers are characterized by a smaller hopping activation energy, possibly reflecting the absence of transport barriers at the inter-fiber contacts. In future studies, the resistance of the fibers might be reduced by, for example, oxidative intercalation of aniline leading to polyaniline bronzes as demonstrated by Wu and coworkers for bulk V_2O_5 xerogels.[28] Another possibility could be the conversion of V_2O_5 into vanadium dioxide (VO_2) via thermal annealing, following the procedure reported by Lu and coworkers for thin films of sol/gel-derived V_2O_5.[29] Similar VO_2 films were shown to exhibit a metal–insulator transition at about 370 K.[30]

Experimental

V_2O_5 sols were prepared from 0.2 g ammonium (meta)vanadate (Aldrich) and 2 g acidic ion exchange resin (DOWEX 50WX8-100, Aldrich) in 40 mL water. After a few hours the formation of an orange sol is observed that darkens with time. V_2O_5 fibers with lengths of a few micrometers were

  0935-9648/00/0603-0423 $ 17.50+.50/0

observed after about 3 days. Sols that were aged for at least 4 weeks were used for the electrical measurements.

Electrode arrays were created on silicon wafers with a 1 μm thick thermally grown oxide layer. Gold electrodes spaced by 3 μm were fabricated by conventional optical lithography. AuPd (40/60) lines with a separation of about 100 nm were defined by e-beam lithography using a two-layer resist and a modified Hitachi S2300 scanning electron microscope.

Before deposition of V_2O_5 fibers, the substrates were silanized for 2 min at room temperature by immersion in a 2.5 mM aqueous solution of 3-aminopropyltriethoxysilane (Aldrich), followed by thorough rinsing with pure water and drying under a stream of air.

V_2O_5 network samples were prepared as follows: A droplet of undiluted V_2O_5 sol, several days old, was deposited on the electrode structure with 3 μm gaps. After 15 min, the samples were rinsed with water and blown dry with air. For deposition of individual fibers on the electrode arrays or on bare substrates prior to e-beam lithography, the aminosilanized substrates were dipped into a mixture of V_2O_5 sol/water (1:10) for 2–3 s. The substrates were then rinsed with water and blown dry.

The samples were characterized with an SFM (Digital Instruments, Nanoscope IIIa) in tapping mode using conventional silicon cantilevers. The electrical transport measurements were performed under vacuum with a Keithley 617 electrometer and a Keithley 230 voltage source. The samples showed stable transport characteristics over several days.

Received: September 22, 1999
Final version: December 14, 1999

[1] S. Frank, P. Poncharal, Z. L. Wang, W. A. de Heer, *Science* **1998**, *280*, 1744
[2] S. J. Tans, A. R. M. Verschueren, C. Dekker, *Nature* **1998**, *393*, 49.
[3] R. Martel, T. Schmidt, H. R. Shea, T. Hertel, P. Avouris, *Appl. Phys. Lett.* **1998**, *73*, 2447.
[4] R. Saito, G. Dresselhaus, M. S. Dresselhaus, *Physical Properties of Carbon Nanotubes*, Imperial College Press, London **1998**.
[5] H. T. Soh, C. F. Quate, A. F. Morpurgo, C. M. Marcus, J. Kong, H. Dai, *Appl. Phys. Lett.* **1999**, *75*, 627.
[6] R. Tenne, L. Margulius, M. Genut, G. Hodes, *Nature* **1992**, *360*, 444.
[7] M. Remškar, Z. Škraba, M. Regula, C. Ballif, R. Sanjinés, F. Lévy, *Adv. Mater.* **1998**, *10*, 246.
[8] Y. Q. Zhu, W. B. Hu, W. K. Hsu, M. Terrones, N. Grobert, T. Karali, H. Terrones, J. P. Hare, P. D. Townsend, H. W. Kroto, D. R. M. Walton, *Adv. Mater.* **1999**, *11*, 844.
[9] H.-W. Fink, C. Schönenberger, *Nature* **1999**, *398*, 407.
[10] M. E. Spahr, P. Bitterli, R. Nesper, M. Müller, F. Krumeich, H. U. Nissen, *Angew. Chem. Int. Ed.* **1998**, *37*, 1263.
[11] J. Livage, *Coord. Chem. Rev.* **1998**, *178–180*, 999.
[12] X. Commeinhes, P. Davidson, C. Bourgaux, J. Livage, *Adv. Mater.* **1997**, *9*, 900.
[13] C. Guestaux, J. Leaut, C. Virey, J. Vial, *US Patent 3 658 573*, **1972**.
[14] T. Yao, Y. Oka, N. Yamamoto, *Mater. Res. Bull.* **1992**, *27*, 669.
[15] J. K. Bailey, G. A. Pozarnsky, M. L. Mecartney, *J. Mater. Res.* **1992**, *7*, 2530.
[16] R. M. Abdel-Latif, *Physica B* **1998**, *254*, 273.
[17] J. Haemers, E. Baetens, J. Vennik, *Phys. Status Solidi A* **1973**, *20*, 381.
[18] M. G. Kanatzidis, C.-G. Wu, *J. Am. Chem. Soc.* **1989**, *111*, 4139.
[19] N. Gharbi, C. Sanchez, J. Livage, J. Lemerle, L. Néjem, J. Lefebvre, *Inorg. Chem.* **1982**, *21*, 2758.
[20] C. T. Gibson, G. S. Watson, S. Myhra, *Scanning Electron Microsc.* **1997**, *19*, 564.
[21] T. Allersma, R. Hakim, T. N. Kennedy, J. D. Mackenzie, *J. Chem. Phys.* **1967**, *46*, 154.
[22] F. P. Koffyberg, F. A. Benko, *Philos. Mag. B* **1978**, *38*, 357.
[23] J. Bullot, P. Cordier, O. Gallais, M. Gauthier, J. Livage, *J. Non-Cryst. Solids* **1984**, *68*, 123.
[24] J. Bullot, O. Gallais, M. Gauthier, J. Livage, *Appl. Phys. Lett.* **1980**, *36*, 986.
[25] J. Livage, *Chem. Mater.* **1991**, *3*, 578.
[26] N. F. Mott, *J. Non-Cryst. Solids* **1968**, *1*, 1.
[27] J. Nygård, D. H. Cobden, M. Bockrath, P. L. McEuen, P. E. Lindelof, *Appl. Phys. A* **1999**, *69*, 297.
[28] C.-G. Wu, D. C. DeGroot, H. O. Marcy, J. L. Schindler, C. R. Kannewurf, Y.-J. Liu, W. Hirpo, M. G. Kanatzidis, *Chem. Mater.* **1996**, *8*, 1992.
[29] S. Lu, L. Hou, F. Gan, *Adv. Mater.* **1997**, *9*, 244.
[30] L. Livage, F. Beteille, C. Roux, M. Chatry, P. Davidson, *Acta Mater.* **1998**, *46*, 743.

Constructive Nanolithography: Site-Defined Silver Self-Assembly on Nanoelectrochemically Patterned Monolayer Templates**

By *Rivka Maoz,* Eli Frydman, Sidney R. Cohen,* and *Jacob Sagiv**

Dedicated to Professor Günther Wulff on the occasion of his 65th birthday

We have recently reported on the possibility of achieving non-destructive surface patterning of a vinyl-terminated silane monolayer self-assembled on silicon, by the application of an electrical bias to a conducting atomic force microscope (AFM) tip operated in normal ambient conditions.[1] The tip-induced transformation was shown to proceed by local electrochemical oxidation of the top vinyl functions of the monolayer, with full preservation of its overall molecular order and structural integrity. It was further shown that such nanoelectrochemically patterned monolayers may be employed as extremely robust, stable templates for the controlled self-assembly of organic bilayer structures with predefined size, shape, and surface location.[1]

Here we show that this template-controlled self-assembly strategy, referred to as *constructive nanolithography,* can be extended to the planned construction of hybrid metal–organic surface nanostructures. Starting with a thiol-top-functionalized silane monolayer (TFSM) with silver ions chemisorbed on its outer surface (Ag^+–TFSM), metallic silver nanoparticles are generated at selected surface sites by either wet chemical or tip-induced electrochemical reduction of the surface-bound metal ions. As illustrated in Figure 1, the conventional wet chemical reduction (e.g., with aqueous $NaBH_4$) can be used to cover macroscopic surface areas, with lateral dimensions from about 0.5 mm[2] to several centimeters, whereas site-defined reduction of the silver thiolate in the micron- down to the nanometer-size range can be achieved with the help of a conducting AFM tip. If desired, larger metal islands and thicker films, useful as electrical contacts and current leads, may be grown by further chemical development of the initially-generated silver particles (Fig. 1). Thus, silver metal structures are assembled according to a predefined design, by non-destructively im-

[*] Dr. R. Maoz, E. Frydman, Prof. J. Sagiv
Department of Materials and Interfaces
The Weizmann Institute of Science
76100 Rehovot (Israel)
Dr. S. R. Cohen
Chemical Services Unit
The Weizmann Institute of Science
76100 Rehovot (Israel)

[**] We are grateful to Dr. Kazufumi Ogawa of Matsushita Electric Industrial Co. (Osaka) for supplying the NTS used in the assembly of the monolayer templates. Support of this research by the MINERVA Foundation, Germany, the "G.M.J. Schmidt Minerva Center on Supramolecular Architectures", and an Eshkol fellowship (EF), Ministry of Science, Jerusalem, are acknowledged.

  0935-9648/00/0603-0424 $ 17.50+.50/0